

LCOS based Flexible Spatial Channel Switch for Heterogeneous SDM Fiber Network

Yuta Goto, Satoshi Shinada, Yusuke Hirota and Hideaki Furukawa

National Institute of Information and Communications Technology (NICT),

4-2-1, Nukui-Kitamachi, Koganei, Tokyo, 184-8795, Japan

y-goto@nict.go.jp

Abstract: We propose an LCOS based flexible spatial channel switch for a heterogeneous SDM fiber network which can easily connect different types of SDM fibers without FIFO. The switching operation was confirmed by measuring OSNR and BER characteristics. © 2022 The Author(s)

1. Introduction

Spatial division multiplexing (SDM) [1] is expected as a candidate technology of the next generation for large capacity optical communication systems. The SDM can increase the transmission capacity by using the SDM fiber such as multi-core fiber (MCF) and multi-mode fiber (MMF), which has multiple spatial channels. On the other hand, the constraint that all fibers of the optical network need to use same type of MCF should be released for open optical network era. So far, some key results of transmission experiment with the various type of SDM fiber are reported [2–5]. Therefore, the next generation optical network can call on the use of those different SDM fibers. To respond this demand, the optical network with the heterogeneous SDM fiber has been proposed and demonstrated [6,7] as shown Fig.1(a). In [6], a network composed of three types of SDM fibers, which has six spatial channels (six parallel single-mode fibers, six mode fiber and six coupled core fibers), has been reported. In [7], a network composed of multiple types of SDM fiber with the different number of spatial channels (7 core fiber, 19 core fiber and 22 core fiber) has been demonstrated. Especially, in [7], each spatial channel is routed by an optical backplane consisting of multiple micro electro mechanical systems (MEMS) switches in each node. However, those nodes connected the heterogeneous SDM fiber requires the various type of the fan-in fan-out (FIFO) devices, which are optimized for each SDM fiber. Furthermore, in the case of spatial switching at a relay node, the port number of the MEMS devices in the optical backplane leads to a proportional increase with the number of spatial channels as shown in Fig. 1(b). This causes the increase of the component count and can be a problem in maintenance management of the network.

To solve this problem, we propose and demonstrate a liquid crystal on silicon (LCOS) based flexible spatial channel switch. This method implements the multi-plane light conversion (MPLC) technology [8] which includes the multiple diffraction effects with the LCOS that is the one of spatial light modulators and realizes the flexible routing of spatial channels including the inter spatial-channel switching, the spatial-channel selective switching and the connection between different types of SDM fibers. The switching speed of LCOS based flexible spatial channel switch is about several tens of milli second due to the operation speed of the LCOS. Although the LCOS is slower than MEMS, our switch can operate at speeds similar to general LCOS based wavelength selective switch. In this paper, we confirm the fundamental switching operation by measuring an optical signal-to-noise ratio (OSNR) characteristic on the C-band. In addition, we confirmed the bit error rate (BER) characteristics of 20 Gbaud 16 value quadrature amplitude modulation (16QAM) signal in each optical path.

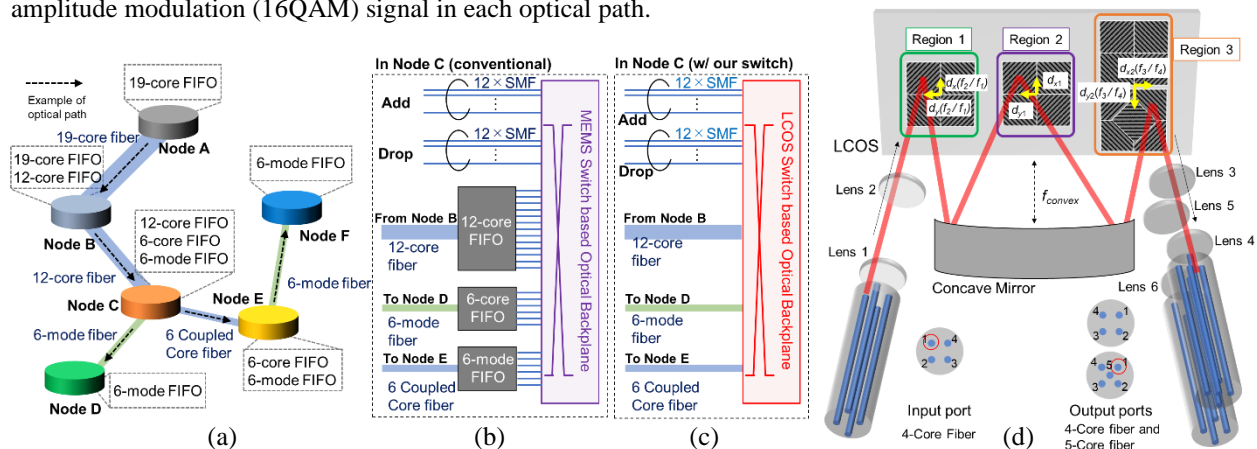


Fig. 1 (a) Example of heterogeneous SDM fiber Network, (b) the configuration of node C with FIFO, (c) the configuration of node C with proposed LCOS based switch, (d) LCOS based flexible spatial channel switch.

2. LCOS based Flexible Spatial Channel Switch

In our switch, a successive (3 time) reflection type MPLC with a concave mirror is adopted. In addition, the phase pattern was not optimized unlike the usual MPLC [8] and was directly calculated as diffraction grating pattern from the inter-core distance, the focal length of the lens, and the distance between the fibers at the output ports.

Here, as an example, we describe the case of the path from core 1 of 4-core fiber of the input port to core 1 of 5-core fiber of the output port in Fig.1(b). The diffraction grating pattern on LCOS can be divided into three regions where are region 1, region 2, and region 3 as shown in Fig. 1(b). First, the light from core 1 of the input port is imaged at the position from the center of the region 1 at $d_x(f_2/f_1)$ along x -axis and at $d_y(f_2/f_1)$ along y -axis, where, d_x and d_y are distances of core 1 from the center of 4-core fiber of input port along x - and y -axis, and f_1 and f_2 are focal length of lens 1 and lens 2. In the region 1, the diffraction grating pattern with diffraction angle of $\theta_{dx1} = \arctan(d_{x1}/f_{concave}) - \theta_{input}$ along x -axis and $\theta_{dy1} = \arctan(d_{y1}/f_{concave}) - \theta_{input}$ along y -axis is displayed, where, θ_{input} is the angle of incidence from the input port to the LCOS, d_{x1} and d_{y1} are the distance from center of region 2 to the upper left position in region 2 along x - and y -axis, and $f_{concave}$ is the focal length of the concave mirror, respectively. Then, the reflected light from the concave mirror is collimated and reached on the upper left position of region 2. Next, in the upper left position in region 2, the diffraction grating pattern with diffraction angle of $\theta_{dx2} = \arctan[\{d_{x2}(f_3/f_4) + d_x(f_2/f_1)\}/f_{concave}]$ along x -axis and $\theta_{dy2} = \arctan[\{d_{y2}(f_3/f_4) + d_y(f_2/f_1)\}/f_{concave}]$ along y -axis is displayed. Where, d_{x2} and d_{y2} are distances of core 3 from center of 5-core fiber of the output port 1, and f_3 and f_4 are focal length of lens 3 and lens 4. Finally, in region 3, the light diffracted from region 3 is focused on the end-face of core 3 of 5-core fiber of the output port by displaying the diffraction grating pattern which cancels θ_{dx1} and θ_{dy1} , i.e., $-\theta_{dx1}$ and $-\theta_{dy1}$ on region 3. By changing the θ_{dx2} and θ_{dy2} , the output can be switched any output port and/or output core.

3. Experiment

The photograph of the LCOS based switch is shown in Fig. 2(a). In the setup, the focal length of the collimator lenses, which correspond to lens 1 and lens 4 in Fig. 1(b), was 5 mm, and the focal length of the condenser lenses, which correspond to lens 2 and lens 3 in Fig.1(b), was 100 mm. Then, θ_{input} and $f_{concave}$ were 2.93 degree and 50 mm. Figure 2 (b) shows diffraction grating pattern displayed on LCOS. This is the enlarged view of a part of region 2. The optical path can be switched by changing images with different fringe intervals. In this experiment, we assumed there are two output ports by moving the fiber and the collimator lens in the output port using z -axis stage as shown in Fig. 3. In addition, we assumed the use of the heterogeneous SDM fiber that has the different core position by swapping the output port 4-core fiber to the single mode fiber (SMF). Here, in the output port, set of two 4-core fiber was defined as "Case 1", and set of 4-core fiber and the SMF was defined as "Case 2" as shown in fig.3. A polarization diversity optics is required to handle the polarization multiplexed signals, but it was omitted due to experimental resource constraints.

First, we measured the insertion loss (IL) and the crosstalk (XT) on the C-band. During measurement, the super continuum light source is sequentially input to each core of input port through the FIFO device. Note that the FIFOs were used for only connecting between the SMF of the measurement instruments and the LCOS based flexible spatial channel switch, not for switching. Since there are 8 outputs (4 cores \times 2 ports) in Case 1, there are 8 optical paths for each core of the input port. Therefore, 64 measurements (8 optical paths \times 8 outputs) are required. At this time, optical output powers of correct destination cores are defined as ILs, and optical output powers of other cores are defined as XTs. In Case 2, there are 5 outputs and 25 measurements. Optical output powers were sequentially measured by an optical spectrum analyzer (OSA). Figure 4 shows all ILs and XTs. According to the results, maximum IL was 24.6 dB to 36.7 dB. Since the FIFOs has the loss of 0.6 dB to 3.0 dB, we can say that the actual IL was 21.6 dB to 36.1 dB. This because that the diffraction efficiency of the grating pattern on LCOS is up to -7.0 dB approximately. The optical loss is accumulated via 3 times diffraction. In addition, the IL was slightly large on the long wavelength side. This is because the diffraction grating pattern displayed on the LCOS causes angular dispersion and the vignetting at the core of output port. On the other hand, very low XTs and the SNR of about 27.0 dB were observed. This large optical loss can be reduced by optimizing the phase pattern on LCOS. In [8], a mode multiplexer with ILs of about 10 dB or less has been reported. In addition, according to Fig.5, we can see the undesired high-order diffracted light was mixed in the XTs. This is due to the high-order diffraction light and may be also suppressed by optimizing the phase pattern of LCOS.

Next, we evaluated the BER versus OSNR characteristics. The setup for the evaluation of BER versus OSNR characteristics is shown in Fig. 2(c). The 20 Gbaud single polarization (SP) 16QAM signals was generated by the arbitrary waveform generator (AWG) of 120 G Samples/s and the SP IQ modulator. The wavelength of CW laser source was 1552.5244 nm, and ILs of that wavelength was 24.4 dB to 34.6 dB. The optical signal was connected to

the LCOS based flexible spatial channel switch by the input FIFO device. Then, the BER of all cores in all output ports was measured by the optical modulation analyzer (OMA) (KEYSIGHT N4391A) of 160 GSamples/s. The BER was estimated by the supplied function of the OMA. Figure 5 shows the BER versus OSNR characteristic. We confirmed the OSNR penalty of each output compared to the back-to-back measurement. This is due to the large IL of about 30 dB. Therefore, this OSNR penalty can be also improved by optimizing the phase pattern on LCOS.

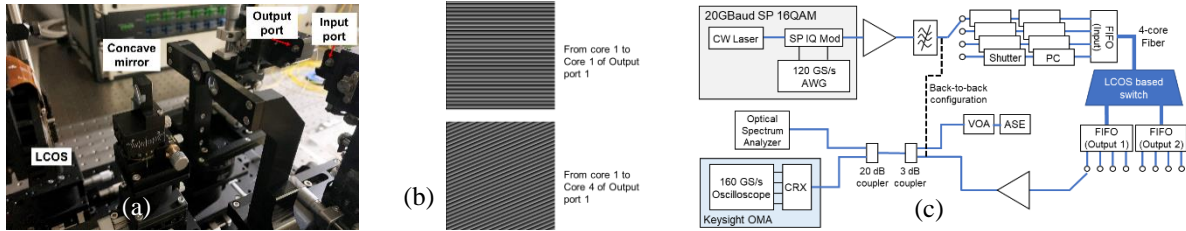


Fig. 2 (a) Photograph of the LCOS based switch, (b) displayed images, (c) experimental setup for BER measurement.

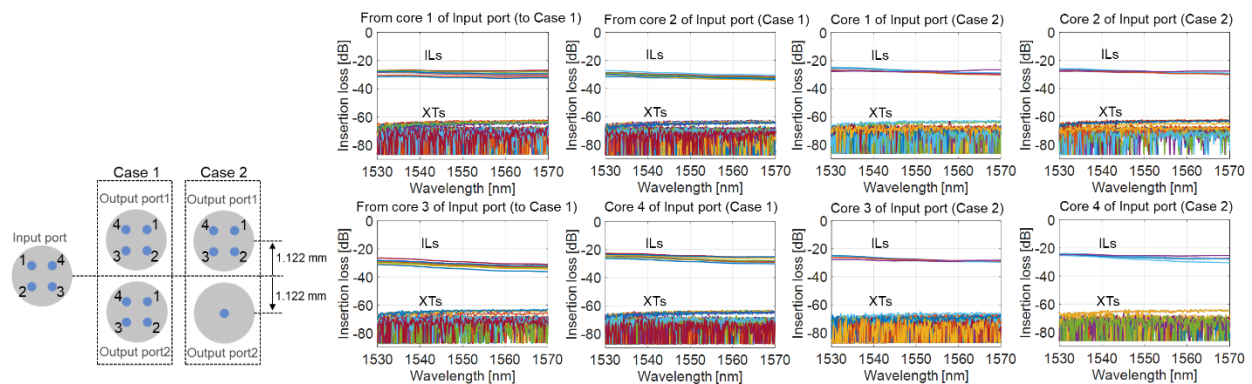


Fig. 3 Layout of each cores.

Fig.4 ILs and XTs in all switching path.

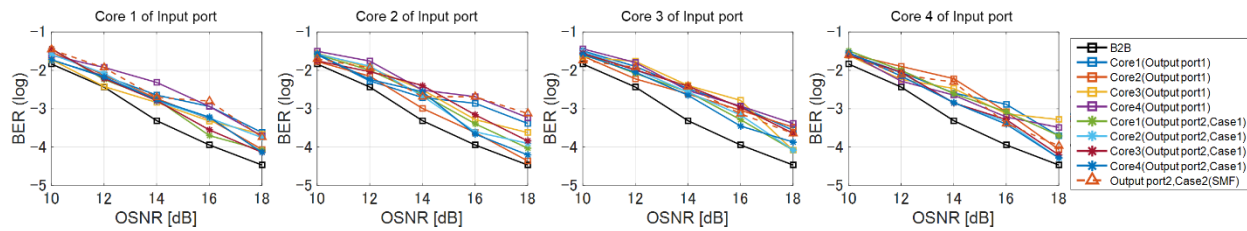


Fig.5 BER versus OSNR characteristics.

4. Conclusion

We proposed and demonstrated the LCOS based flexible spatial channel switch without FIFO for the heterogeneous SDM fiber network. In the experiment, we confirmed the fundamental switching operation by measuring IL, XT and BER characteristics. In the future, we will show that our switch can adapt to the various type of MCFs more than 10 cores by using the unallocated area of LCOS. Furthermore, by optimizing the phase pattern on LCOS similar to [8], we can reduce the IL and the OSNR penalty of the BER and can show that our switch can handle the SDM fiber included the complicated spatial channels such as coupled core or spatial modes.

Reference

- [1] D. Richardson *et al.*, "Space-division multiplexing in optical fibres", *Nature Photon* **7**, 354-362 (2013).
- [2] D. Soma *et al.*, "10.16 Peta-bit/s Dense SDM/WDM transmission over Low-DMD 6-Mode 19-Core Fibre Across C+L Band," *ECOC2017*, pp. 1-3.
- [3] G. Rademacher *et al.*, "10.66 Peta-Bit/s Transmission over a 38-Core-Three-Mode Fiber," *OFC2020*, pp. 1-3.
- [4] B. J. Puttnam *et al.*, "1 Pb/s Transmission in a 125µm diameter 4-core MCF," *CLEO2020*, pp. 1-2.
- [5] J. Sakaguchi *et al.*, "19-core MCF transmission system using EDFA with shared core pumping coupled in free-space optics," *ECOC2013*, pp. 1-3.
- [6] N. K. Fontaine *et al.*, "Heterogeneous space-division multiplexing and joint wavelength switching demonstration," *OFC2015*, pp. 1-3.
- [7] G. M. Saridis *et al.*, "Experimental Demonstration of a Flexible Filterless and Bidirectional SDM Optical Metro/Inter-DC Network," *ECOC2016*, pp. 1-3.
- [8] G. Labroille *et al.*, "Mode selective 10-mode multiplexer based on multi-plane light conversion," *OFC2016*, pp. 1-3.